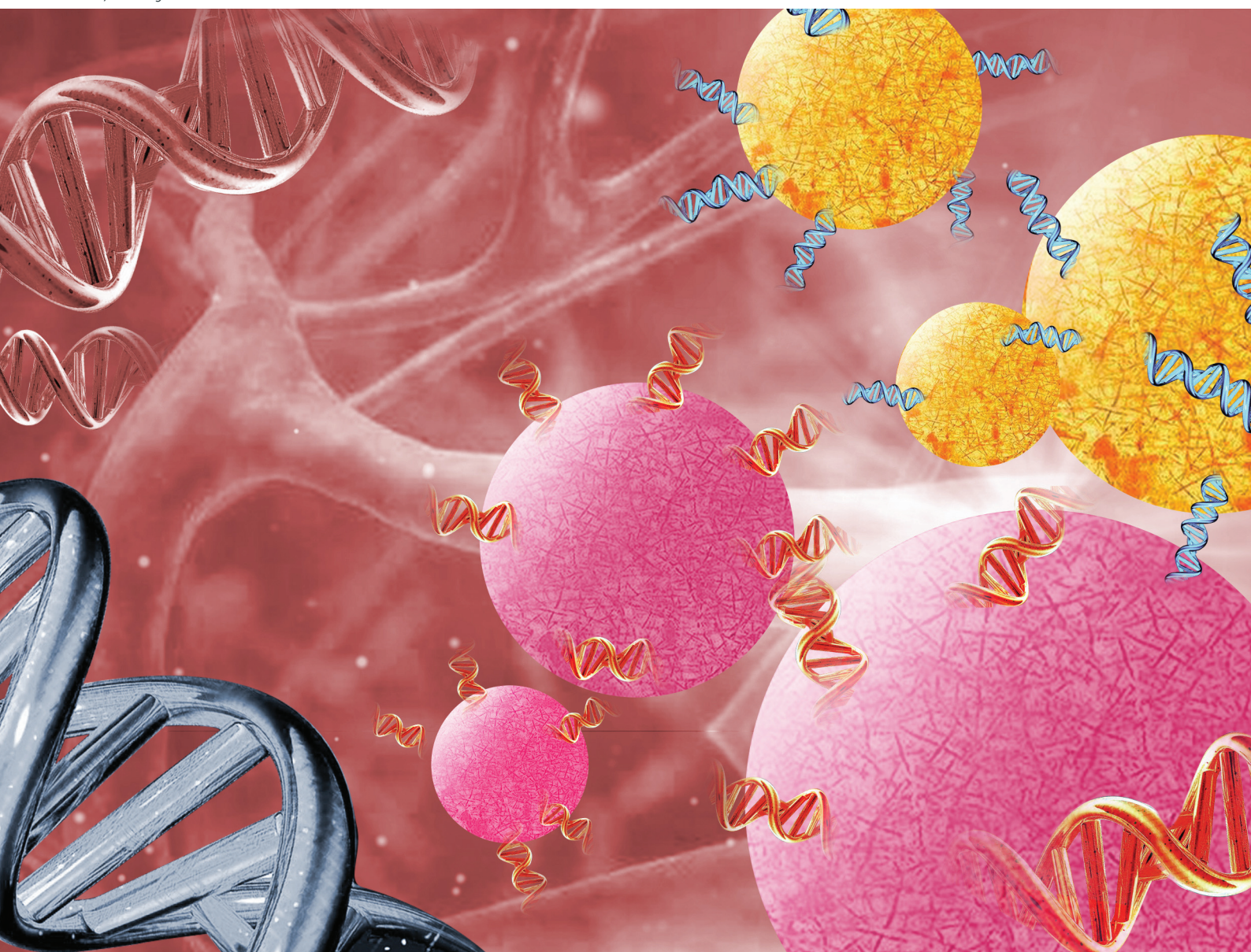


Analyst

rsc.li/analyst



ISSN 0003-2654

COMMUNICATION

Bo Zhang, Dongliang Ge *et al.*
High-resolution DNA size enrichment using a magnetic
nano-platform and application in non-invasive
prenatal testing



Cite this: *Analyst*, 2020, **145**, 5733

Received 23rd April 2020,

Accepted 1st July 2020

DOI: 10.1039/d0an00813c

rsc.li/analyst

High-resolution DNA size enrichment using a magnetic nano-platform and application in non-invasive prenatal testing†

Bo Zhang,^{ib} *‡^{a,b,c} Shuting Zhao,^{‡a,c} Hao Wan,^{‡a} Ying Liu,^{‡b} Fei Zhang,^{‡b,d} Xin Guo,^{‡a,b,c} Wenqi Zeng,^{a,c} Haiyan Zhang,^b Linghua Zeng,^b Jiale Qu,^c Ben-Qing Wu,^e Xinhong Wan,^f Charles R. Cantor^{a,g} and Dongliang Ge^{*a,b,c}

Precise DNA sizing can boost sequencing efficiency, reduce cost, improve data quality, and even allow sequencing of low-input samples, while current pervasive DNA sizing approaches are incapable of differentiating DNA fragments under 200 bp with high resolution (<20 bp). In non-invasive prenatal testing (NIPT), the size distribution of cell-free fetal DNA in maternal plasma (main peak at 143 bp) is significantly different from that of maternal cell-free DNA (main peak at 166 bp). The current pervasive workflow of NIPT and DNA sizing is unable to take advantage of this 20 bp difference, resulting in sample rejection, test inaccuracy, and restricted clinical utility. Here we report a simple, automatable, high-resolution DNA size enrichment workflow, named MiniEnrich, on a magnetic nano-platform to exploit this 20 bp size difference and to enrich fetal DNA fragments from maternal blood. Two types of magnetic nanoparticles were developed, with one able to filter high-molecular-weight DNA with high resolution and the other able to recover the remaining DNA fragments under the size threshold of interest with >95% yield. Using this method, the average fetal fraction was increased from 13% to 20% after the enrichment, as measured by plasma DNA sequencing. This approach provides a new tool for high-resolution DNA size enrichment under 200 bp, which may improve NIPT accuracy by rescuing rejected non-reportable clinical samples, and enable NIPT earlier in pregnancy. It also has the potential to improve non-invasive screening for fetal monogenic disorders, differentiate tumor-

related DNA in liquid biopsy and find more applications in autoimmune disease diagnosis.

Introduction

Circulating cell-free DNA (cfDNA) is an important source material for non-invasive prenatal testing (NIPT) and tumor liquid biopsies. The discovery of circulating cell-free fetal DNA (cffDNA) in maternal plasma in 1997 by Dennis Lo and his collaborators enabled NIPT of the common fetal chromosomal aneuploidies.^{1–4} NIPT is more sensitive and specific than traditional maternal serum screening for trisomy 21, 18 and 13,^{5–10} and is increasingly being used for screening for sex chromosome aneuploidies and microdeletions.^{11–14} Conventional NIPT by shotgun sequencing (NGS) of cfDNA in maternal plasma starts from the 10th gestational week since it requires at least 4% fetal DNA fraction.¹⁵ Lower fetal DNA fractions introduce high background noise and may lead to false-negative results for common chromosomal abnormalities.¹⁶

cfDNA isolated from maternal plasma has a size distribution ranging from 80 to 1000 bp, where the short fragments (*i.e.* <150 bp) are usually significantly less abundant than the long fragments. The long and short cfDNA in maternal plasma are not randomly fragmented: high-resolution plasma DNA size profiling by paired-end DNA sequencing reveals that the main cfDNA peak is at 166 bp, and the distribution shows a 10 bp periodicity below 150 bp.¹⁵ Compared with maternal cfDNA (mostly originating from the hematopoietic system),^{16–18} the cffDNA in maternal plasma (mostly originating from placental tissues) is shorter.¹⁹ The main peak shifts from 166 bp (maternal) to 143 bp (fetal).²⁰ If this subtle variation could be exploited by enriching cfDNA below 150 bp, we could potentially increase the percentage of fetal DNA, and improve NIPT by rescuing failed samples or enabling NIPT earlier in pregnancy.

Traditional DNA size separation approaches are mostly based on chromatography or electrophoresis,^{21–28} whose

^aApostle Inc., San Jose, CA 95134, USA. E-mail: bzhang@apostlebio.com, dge@apostlebio.com

^bSchool of Innovation and Entrepreneurship, Southern University of Science and Technology, Shenzhen, Guangdong, 518000, China

^cShenzhen Apostle-Sustech Ltd, Shenzhen, Guangdong, 518000, China

^dSchool of Public Health, Southeast University, Nanjing 210009, China

^eDepartment of Pediatrics, University of Chinese Academy of Sciences-Shenzhen Hospital, ShenzhenGuangdong, 518000, China

^fLonggang District Maternity and Child Healthcare Hospital, Shenzhen, Guangdong, 518000, China

^gDepartment of Biomedical Engineering, Boston University, Boston, MA 02215, USA

†Electronic supplementary information (ESI) available. See DOI: 10.1039/d0an00813c

‡These authors contributed equally to this work.

tedious operation limits their clinical and industrial applications. Some other methods for DNA size selection often have a cut-off of 300 bp or higher with low resolution, limiting the application in cfDNA studies.

Here, we describe a novel DNA size enrichment approach based on a magnetic nano-platform, named MiniEnrich, to realize DNA size separation with 20 bp resolution and high yield below 200 bp. We explored its application in fetal DNA fragment enrichment in maternal plasma. This workflow can separate short fragments from long fragments with high resolution and therefore significantly increase the relative percentage of short fragments, which could potentially improve the sensitivity and accuracy of NIPT and demonstrate potential in other clinical diagnosis fields (*i.e.* liquid biopsy and autoimmune diseases).

Results and discussion

MiniEnrich is a magnetic nano-platform, employing two types of magnetic nanoparticles and the corresponding cfDNA selection chemistry (Fig. 1). The cfDNA mixture is first mixed with carboxyl nanoparticles (Substrate A) which capture cfDNA with a size over a defined threshold in the presence of polyethylene glycol (PEG) as the crowding agent. The supernatant is separated from Substrate A and mixed with hydroxyl nanoparticles (Substrate B) which efficiently capture the remaining cfDNA with a size below the defined threshold in the presence of isopropanol. The cfDNA captured on Substrate A and Substrate B

can then be individually washed and eluted, resulting in enriched cfDNA above or below this defined size threshold.

The data generated using a synthetic DNA ladder from 20 to 1000 bp show that Substrate A is efficient at capturing cfDNA above 200 bp (Fig. 2A) and Substrate B is efficient at capturing the remaining cfDNA in the supernatant, including DNA as short as 20 bp (Fig. 2B). By combining these two substrates, short and long DNA fragments can be separated and DNA fragments of interest (long or short) can be enriched with high yield. To further tune the possible thresholds for different applications, we explored different size thresholds by changing the volume ratio of Substrate A to the sample. Here we used a commercial cfDNA standard for demonstration and performed the enrichment workflow with gradually increasing volumes of Substrate A. The volume ratio of Substrate A is used to adjust the size threshold in the narrow window between 150 bp and 200 bp, and the corresponding DNA recovered by Substrate B is finely tuned (Fig. 3A). As the Substrate A-to-sample volume ratio increased from 1.2 to 1.8, the percentage of cfDNA below 150 bp increased from 45% to 92% (Fig. 3B), and the average cfDNA length of the enriched short fragment portion decreased from 176 bp to 96 bp (Fig. 3C).

To investigate whether the enriched short fragments by the MiniEnrich workflow can improve the fetal fraction (FF) in NIPT, we obtained plasma samples from 10 pregnant women with gestation times spanning from 16 weeks to 38 weeks and then identified 5 pregnant women carrying male fetuses by Y chromosome-based qPCR assay of their cfDNA (plasma samples obtained from the Department of Pediatrics, University of Chinese Academy of Sciences-Shenzhen Hospital,

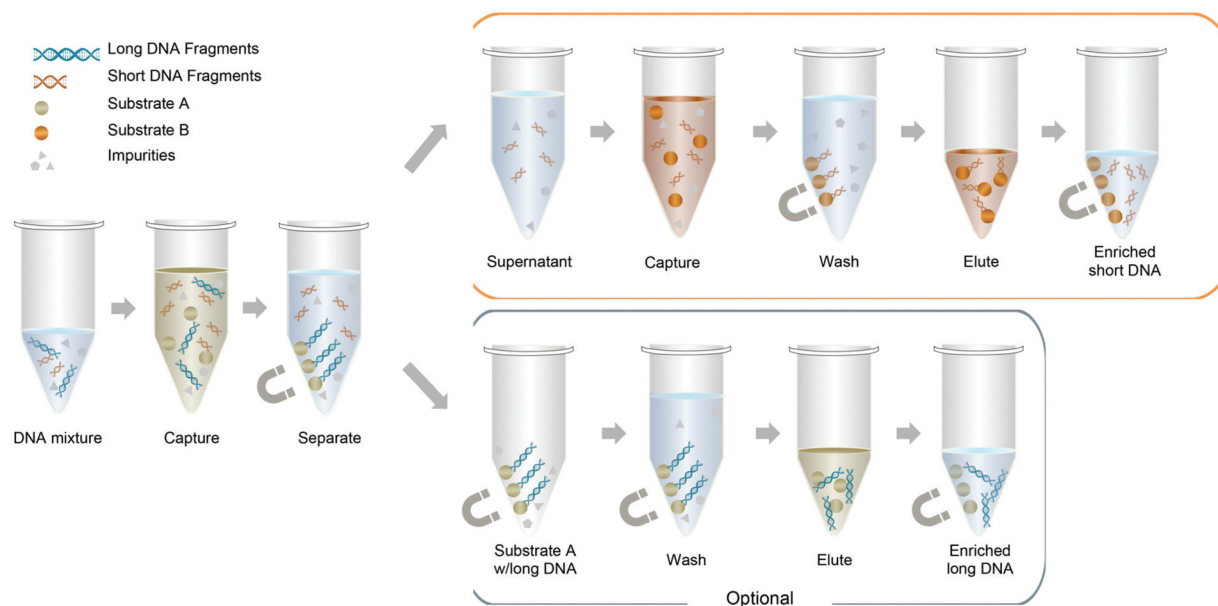


Fig. 1 Workflow to preferentially separate short DNA fragments. DNA fragments of various sizes are first mixed with Substrate A (*e.g.* magnetic beads), which preferentially captures long fragments. The long fragments are separated from the short fragments by an external force (*e.g.* a magnetic field). The short fragments together with impurities remaining in the supernatant are then transferred to a new tube, where the short fragments are captured by Substrate B (*e.g.* a different kind of magnetic bead). After washing off the impurities, the short fragments are eluted from Substrate B and used for the downstream assays. Optionally, the long fragments can be collected by eluting from Substrate A after the washing step.

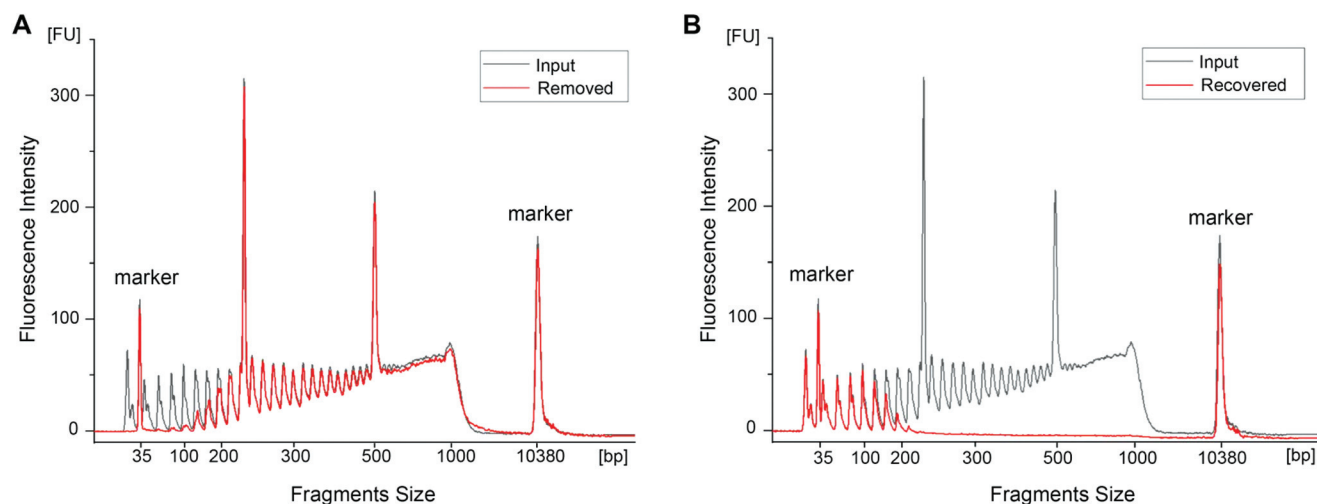


Fig. 2 Removal and recovery of different-sized DNA fragments by Substrate A and Substrate B. A synthetic DNA ladder from 20 to 1000 bp DNA fragments was first mixed with Substrate A to remove the long fragments >200 bp; then the supernatant was mixed with Substrate B to recover the small fragments <200 bp. The eluted fragments were analyzed using an Agilent Bioanalyzer 2100 after spiking with a marker. (A) The eluate from Substrate A (red) was compared with the input DNA fragments (black), showing that the long DNA fragments (200–1000 bp) are successfully removed. (B) The eluate from Substrate B (red) compared with the input DNA fragments (black) showed the efficient recovery of short DNA fragments, as short as 20 bp. The upper and lower internal markers of the Agilent Bioanalyzer are used for size alignment and quantitation during the characterization. By combining the two steps, preferential selection of short DNA fragments is achieved.

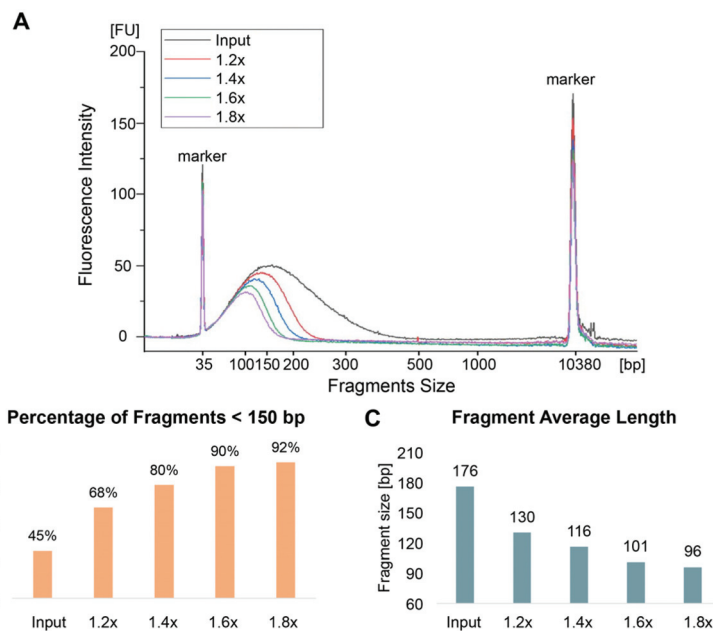


Fig. 3 Tuning thresholds for enriching short DNA fragments by customized Substrate A volume. A commercial cfDNA standard (35–500 bp) was processed to enrich the short fragments. The ratio of Substrate A volume to sample volume was varied. (A) Agilent Bioanalyzer results for 1.2x, 1.4x, 1.6x and 1.8x versus original DNA input (grey curve). Quantitative analysis of the enriched samples shows (B) the fraction of DNA < 150 bp and (C) the average length of DNA. Changing the ratio of Substrate A volume to sample volume clearly affects the size of the enriched product.

Shenzhen, China). We performed the MiniEnrich workflow to enrich short fragments for the isolated cfDNA from the plasma of these 5 pregnant women carrying male fetuses, as the Y chromosome can be used to calculate the fetal fraction by the established bioinformatics pipeline. In brief, based on the results in Fig. 3, a 1.6-fold ratio of Substrate A volume to

sample volume was used for the optimized recovery of DNA < 150 bp, which is presumably the threshold for fetus-specific cfDNA from the literature.²⁰ 10⁶ paired-end whole genome shotgun sequencing (WGS) was performed on the 5 enriched cfDNA samples and the corresponding 5 cfDNA reference samples without the enrichment workflow. The FF before and

after enrichment was calculated using the DEFRAG approach.^{29,30} Measurements of the GC content and the copy numbers of chromosomes 13, 18, and 21 before and after enrichment showed that the MiniEnrich process does not lead to bias to downstream WGS (ESI Fig. 1 and 2†).

The fragment sizes measured by WGS are plotted in Fig. 4A, showing a consistent shift of the cfDNA peak from 170 bp to 150 bp after enrichment for all 5 samples. On average, the percentage of DNA fragments <150 bp increased from 13.7% to 44.5% after the enrichment (Fig. 4B), indicating the successful enrichment of DNA fragments <150 bp. The profile of short fragments produced by the MiniEnrich workflow is highly consistent with the reported fragmentation profile of fetal DNA determined by examining sequences containing obligatory paternal DNA sequences,²⁰ demonstrating the potential enrichment of the fetal DNA fraction. The FF calculated using the DEFRAG approach shows that there is a significant and consistent increase in the FF after the MiniEnrich process for all 5 samples (Fig. 4C). The average change of the FF is 7%, with a minimal FF change of 4.7% and the highest FF change of 9.2% (Fig. 4D). This 7% average change introduced by the MiniEnrich approach has the potential to rescue rejected non-reportable clinical samples by bringing the fetal fraction above the detection limit (usually 4%), as cfDNA samples with the fetal fraction less than 4% generally lead to inconclusive reports, due to pregnancies earlier than the 10th gestational week, or with increased maternal weight.¹⁵

In addition to that, the MiniEnrich workflow potentially can be used to enable NIPT at earlier stages. The cffDNA concentration usually increases with the gestation time as reported in the literature, and this trend was observed in the 5 samples we investigated (Fig. 5).¹⁵ Linear regression was modeled to estimate the likely FF earlier in gestation and the FF would reach 4% at week 6.5, earlier than the 10th week as the current requirement in NIPT.

To further validate the potential NIPT application of the MiniEnrich workflow in different downstream assays other than 10× WGS, we utilized the ddPCR platform to characterize cffDNA before and after the MiniEnrich workflow from an additional 14 plasma samples from pregnant women carrying male fetuses, among which 10 were below 20-week gestational age (plasma samples obtained from Longgang District Maternity and Child Healthcare Hospital, Shenzhen, China). By comparing the copy numbers detected by ddPCR, we found a median 2.35-fold increase of chromosome Y percentage after the MiniEnrich workflow, showing the similar trend of the increased fetal fraction (ESI Table 1†).

The discovery of cffDNA in maternal plasma in 1997 led to the widespread use of NIPT¹ for common chromosomal aneuploidies, sex chromosomal aneuploidies and microdeletions.^{5–14} A low fetal DNA fraction introduces significant background noise and can lead to false-negative screening results. For pregnancies with the FF too low for standard NIPT procedures, computational tools may be used to increase the

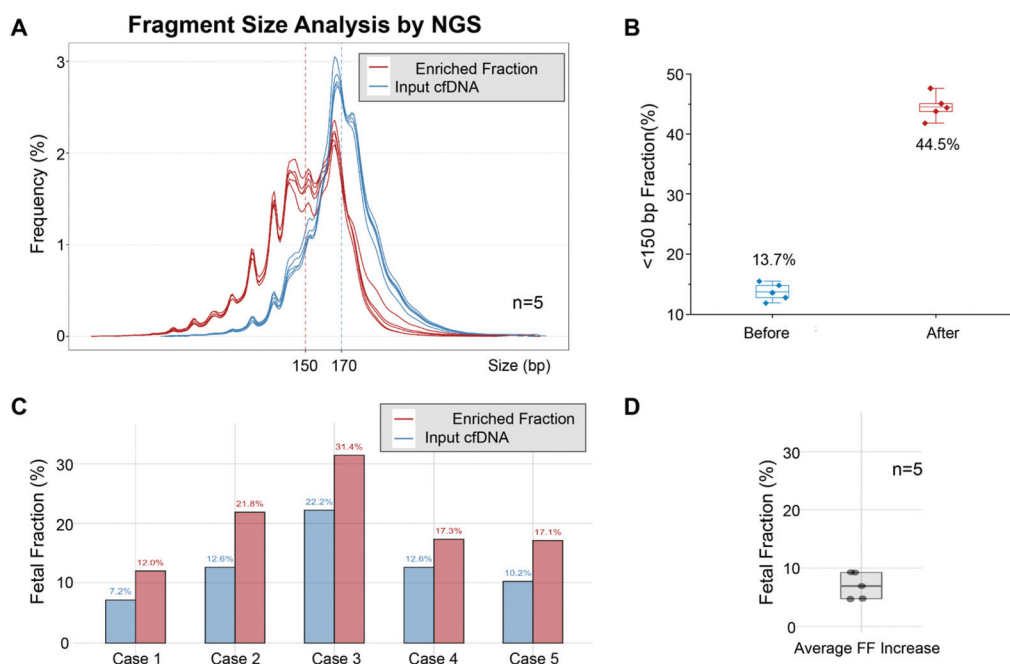


Fig. 4 NGS fragment size analysis and the fetal fraction (FF) before and after the MiniEnrich workflow. Five clinical samples of maternal plasma were processed to enrich the short fragments using the MiniEnrich workflow. (A) Compared to the input cfDNA (before enrichment, blue), the peak of the enriched DNA fraction in 170 bp decreased to 150 bp (after enrichment, red) with an increase in the proportion <150 bp. (B) Quantitative analyses of the enriched samples show the average increase in the fraction of DNA <150 bp. (C) Increase in the fetal fraction after enrichment for five samples and (D) average increase in the fetal fraction (%).

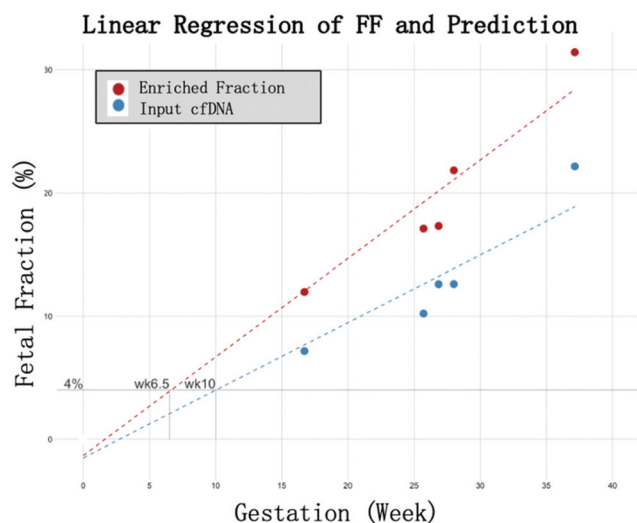


Fig. 5 The fetal fraction before and after the MiniEnrich workflow and the linear regression model to predict the FF at earlier gestation weeks. The gestation time and fetal DNA fraction of 5 clinical samples of maternal plasma before and after enrichment plotted shows the increased FF with longer gestation time. A linear regression model was used to estimate the FF with the MiniEnrich workflow which would reach 4% at week 6.5, earlier than the 10th week as the current requirement in NIPT.

effective FF in some cases,^{31–34} but they have limitations in cost, efficiency, sensitivity and specificity. Some other methods are developed for size selection purpose, often with the cutoff of 300 bp or higher,³⁵ due to the limited resolution to separate fetal and maternal cfDNA under 200 bp. The limited resolution of some previous methods also causes a significant reduction of input cfDNA and could be a major concern for downstream assays. Compared to a study that reported 91.76% reduction of cfDNA after the size separation,³⁶ the MiniEnrich workflow achieved a recovery of 31.59% input cfDNA after the enrichment workflow, showing its feasibility for NIPT and other applications. The efficient recovery and high resolution of the MiniEnrich workflow are mainly achieved by the uniform and small size of nanoparticles as well as their rich surface chemistry. Specifically, during the process of long DNA fragment binding, the uniform size and rich carboxylic surface modification of Substrate A (ESI Fig. 3†) contribute to the consistent and size-specific binding, resulting in the high resolution in the size separation, while the small size of Substrate B provides a large surface area and fast kinetics which are critical for short DNA fragment binding. These two types of magnetic nanoparticles, one able to filter high-molecular-weight DNA and the other able to recover small DNA fragments, together were able to separate DNA fragments under 200 bp with high resolution and yield. By applying the combination of two types of nanoparticles with different surface chemistries, we are able to separate and recover each portion of DNA fragments with higher resolution and yield for the first time, instead of solely removing the long fragments with low size resolution as some methods have reported.³⁶ The recovered long or short frag-

ments by the MiniEnrich workflow can be used for both commercial and in-house downstream assays.

In addition, as a magnetic nano-platform, the MiniEnrich workflow is much easier to operate in common clinical laboratory settings and can be easily automated, and therefore feasible to be incorporated into a mature or scaled-up NIPT workflow. In contrast, previous methods for size separation purpose were mostly based on chromatography or electrophoresis,^{21–28} which are complex or tedious to be widely adopted, limiting their application in clinical settings. For example, gel-based electrophoresis, gel cutting and gel purification are time-consuming and labor-intensive processes. Furthermore, the MiniEnrich workflow has the flexibility to be incorporated into current workflows and downstream assays where high-resolution size separation is desired. In this study, we applied the MiniEnrich workflow after cfDNA isolation, so that the enriched portion (short or long fragments) can be eluted in common elution buffers like Tris-EDTA buffer or H₂O, and can be directly used for various downstream assays including but not limited to NGS, PCR, ddPCR, *etc.*, as the MiniEnrich workflow does not introduce impurities or new substrates in the eluate. This shows advantages over methods which introduce other undesirable components (*e.g.* PEG, salts), which can affect downstream workflows.³⁶

As a universal platform with a customized threshold, the MiniEnrich workflow has the potential to be applied to other applications. For example, current NIPT mostly targets the detection of fetal chromosomal abnormalities. Screening for monogenic disorders such as those associated with *de novo* mutations is not generally available despite their relatively high incidence.³⁷ Increasing the proportion of fetal DNA, by the simple MiniEnrich method described here, may potentially improve the screening of monogenic disorders. Furthermore, this process could also be broadly used to differentiate long and short DNA fragments in other research fields. In liquid biopsy, researchers have reported that cancer patients had altered fragmentation profiles compared with healthy individuals, and the ratio of short-to-long cfDNA could be used to identify cancers and tissue of origin for liquid biopsy purpose.^{38,39} For autoimmune diseases, such as systemic lupus erythematosus (SLE), SLE patients usually have IgG-bound DNA fragments which are much shorter than non-IgG-bound DNA fragments of healthy individuals.⁴⁰ Therefore, the MiniEnrich nanoplatform has great potential as a simple tool for basic research as well as early clinical diagnosis of cancer and immune diseases like SLE.

Conclusions

The MiniEnrich workflow can achieve the enrichment of a sub-population of cfDNA, especially the short cfDNA portion with high recovery and high resolution. Here we demonstrated the significant increase of the fetal fraction after the MiniEnrich process, which could potentially improve NIPT by rescuing non-reportable samples and enabling NIPT at an earlier stage.

It can also be used to facilitate monogenic disease detection in NIPT, or as the tool for other applications involving the size difference of DNA fragments.

Author contributions

B. Z., D. G. and S. Z. conceived the study. B. Z., S. Z., H. W., Y. L. and F. Z. designed the experiments. X. W. and B. W. provided clinical samples. B. Z., S. Z., Y. L., F. Z., H. Z., L. Z. and J. Q. conducted the experiments. B. Z., S. Z., Y. L., X. G., W. Z. and C. R. C. analyzed the data and wrote the manuscript.

Conflicts of interest

C. R. C. is a scientific adviser and an equity holder of Apostle Inc., and served as a consultant for this work. D. G., B. Z., X. G., W. Z., H. W. and S. Z. are employees and equity holders in Apostle Inc.

Acknowledgements

This study was supported by Shenzhen Fundamental Research Funding (JCY20180504165657443 to B. Z., F. Z., H. Z., B. W. and D. G.) and the Science and Technology Innovation Committee of Shenzhen (JCYJ20140414124506130 to X. W.).

References

- 1 Y. M. D. Lo, N. Corbetta, P. F. Chamberlain, V. Rai, I. L. Sargent, C. W. G. Redman and J. S. Wainscoat, *Lancet*, 1997, **350**, 485–487.
- 2 Y. M. D. Lo, M. S. C. Tein, T. K. Lau, C. J. Haines, T. N. Leung, P. M. K. Poon, J. S. Wainscoat, P. J. Johnson, A. M. Z. Chang and N. M. Hjelm, *Am. J. Hum. Genet.*, 1998, **62**, 768–775.
- 3 R. W. K. Chiu, K. C. A. Chan, Y. Gao, V. Y. M. Lau, W. Zheng, T. Y. Leung, C. H. F. Foo, B. Xie, N. B. Y. Tsui, F. M. F. Lun, B. C. Y. Zee, T. K. Lau, C. R. Cantor and Y. M. D. Lo, *Proc. Natl. Acad. Sci. U. S. A.*, 2008, **105**, 20458–20463.
- 4 H. C. Fan, Y. J. Blumenfeld, U. Chitkara, L. Hudgins and S. R. Quake, *Proc. Natl. Acad. Sci. U. S. A.*, 2008, **105**, 16266–16271.
- 5 M. E. Norton, B. Jacobsson, G. K. Swamy, L. C. Laurent, A. C. W. Tomlinson, L. Pereira, J. L. Spitz, D. Hollemon, H. Cuckle and T. J. Musci, *N. Engl. J. Med.*, 2015, **372**, 1589–15897.
- 6 K. Sun, K. C. A. Chan, I. Hudecova, R. W. K. Chiu, Y. M. D. Lo and P. Jiang, *Prenatal Diagn.*, 2017, **37**, 336–340.
- 7 L. Zhang, Q. Zhu, H. Wang and S. Liu, *Am. J. Transl. Res.*, 2017, **9**, 3469–3473.
- 8 X. Sun, J. Lu and X. Ma, *PLoS One*, 2019, **14**(4), e0215368.
- 9 K. Sun, F. M. F. Lun, T. Y. Leung, R. W. K. Chiu, Y. M. D. Lo and H. Sun, *Prenatal Diagn.*, 2018, **38**, 196–203.
- 10 L. S. Chitty, M. Hill, H. White, D. Wright and S. Morris, *Am. J. Obstet. Gynecol.*, 2012, **206**(4), 269–275.
- 11 A. K. Petersen, S. W. Cheung, J. L. Smith, W. Bi, P. A. Ward, S. Peacock, A. Braxton, IB. V. D. Veyver and A. M. Breman, *Am. J. Obstet. Gynecol.*, 2017, **217**, 691.e1.
- 12 L. S. Chitty and Y. M. D. Lo, *Cold Spring Harbor Perspect. Med.*, 2015, **5**, a023085.
- 13 P. K. Agatasa, M. B. Mercer, A. C. Leek, M. B. Smith, E. Philipson and R. M. Farrell, *Prenatal Diagn.*, 2015, **35**, 692–698.
- 14 K. K. Lo, E. Karampetsou, C. Boustred, F. McKay, S. Mason, M. Hill, V. Plagnol and L. S. Chitty, *Am. J. Hum. Genet.*, 2016, **98**, 34–44.
- 15 E. Wang, A. Batey, C. Struble, T. Musci, K. Song and A. Oliphant, *Prenatal Diagn.*, 2013, **33**, 662–666.
- 16 K. Sun, P. Jiang, K. C. A. Chan, J. Wong, Y. K. Y. Cheng, R. H. S. Liang, W. Chan, E. S. K. Ma, S. L. Chan, S. H. Cheng, R. W. Y. Chan, Y. K. Tong, S. S. M. Ng, R. S. M. Wong, D. S. C. Hui, T. N. Leung, T. Y. Leung, P. B. S. Lai, R. W. K. Chiu and Y. M. D. Lo, *Proc. Natl. Acad. Sci. U. S. A.*, 2015, **112**, E5503–E5512.
- 17 Y. Y. N. Lui, K. W. Chik, R. W. K. Chiu, C. Y. Ho, C. W. K. Lam and Y. M. D. Lo, *Clin. Chem.*, 2002, **48**, 421–427.
- 18 K. C. A. Chan, J. Zhang, A. B. Y. Hui, N. Wong, T. K. Lau, T. N. Leung, K. W. Lo, D. W. S. Huang and Y. M. D. Lo, *Clin. Chem.*, 2004, **50**, 88–92.
- 19 S. S. C. Chim, Y. K. Tong, R. W. K. Chiu, T. K. Lau, T. N. Leung, L. Y. S. Chan, C. B. M. Oudejans, C. Ding and Y. M. D. Lo, *Proc. Natl. Acad. Sci. U. S. A.*, 2005, **102**, 14753–14758.
- 20 Y. M. D. Lo, K. C. A. Chan, H. Sun, E. Z. Chen, P. Jiang, F. M. F. Lun, Y. W. Zheng, T. Y. Leung, T. K. Lau, C. R. Cantor and R. W. K. Chiu, *Sci. Transl. Med.*, 2010, **2**(61), 61–69.
- 21 K. H. Hecker, S. M. Green and K. Kobayashi, *J. Biochem. Biophys. Methods*, 2000, **46**(1–2), 83–93.
- 22 M. Du, J. H. Flanagan, B. Lin and Y. Ma, *Electrophoresis*, 2003, **24**(18), 3147–3153.
- 23 R. Lin, D. T. Burke and M. A. Burns, *J. Chromatogr. A*, 2003, **1010**(2), 55–68.
- 24 F. Xu, M. Jabasini, S. Liu and Y. Baba, *Analyst*, 2003, **128**(6), 589–592.
- 25 M. A. Teters, S. E. Conrardy, B. L. Thomas, T. W. Root and E. N. Lightfoot, *J. Chromatogr. A*, 2003, **989**(1), 165–173.
- 26 L. Raptis and H. A. Menard, *J. Clin. Invest.*, 1980, **6**(6), 1391–1399.
- 27 J. Han and H. G. Craighead, *Anal. Chem.*, 2002, **74**(2), 394–401.
- 28 L. Qiao, B. Yu, Y. Liang, C. Zhang, X. Wu, Y. Xue, C. Shen, Q. He, J. Lu, J. Xiang, H. Li, Q. Zheng and T. Wang, *Am. J. Obstet. Gynecol.*, 2019, **221**(4), 345.e1.
- 29 D. M. Beek, R. Straver, M. M. Weiss, E. M. J. Boon, K. H. Amsterdam, C. B. M. Oudejans, M. J. T. Reinders and E. A. Sistermans, *Prenatal Diagn.*, 2017, **37**(8), 769–773.

- 30 M. S. Hestand, M. Bessem, P. Rijn, R. X. Menezes, D. Sie, I. Bakker, E. M. J. Boon, E. A. Sistermans and M. M. Weiss, *Eur. J. Hum. Genet.*, 2019, **27**(2), 198–202.
- 31 T. Mckanna, A. Ryan, S. K. S. Kareht, K. Marchand, C. Grabarits, M. Ali, A. McElheny, K. Gardiner, K. LeChien, M. Hsu, D. Saltzman, M. Stosic, K. Martin and P. Benn, *Ultrasound Obstet. Gynecol.*, 2019, **53**, 73–79.
- 32 J. Zhang, J. Li, J. B. Saucier, Y. Feng, Y. Jiang, J. Sinson, A. K. McCombs, E. S. Schmitt, S. Peacock, S. Chen, H. Dai, X. Ge, G. Wang, C. A. Shaw, H. Mei, A. Breman, F. Xia, Y. Yang, A. Purgason, A. Pourpak, Z. Chen, X. Wang, Y. Wang, S. Kulkarni, K. W. Choy, R. J. Wapner, I. B. V. Veyver, A. Beaudet, S. Parmar, L. J. Wong and C. M. Eng, *Nat. Med.*, 2019, **25**(3), 439–447.
- 33 H. Hong, L. Xu and W. Tong, *Adv. Exp. Med. Biol.*, 2010, **680**, 355–360.
- 34 K. Sun, F. M. F. Lun, T. Y. Leung, R. W. K. Chiu, Y. M. D. Lo and H. Sun, *Prenatal Diagn.*, 2018, **38**(3), 196–203.
- 35 Y. Li, B. Zimmermann, C. Rusterholz, A. Kang, W. Holzgreve and S. Hahn, *Clin. Chem.*, 2004, **50**(6), 1002–1011.
- 36 P. Hu, D. Liang, Y. Chen, Y. Lin, F. Qiao, H. Li, T. Wang, C. Peng, D. Luo, H. Liu and Z. Xu, *J. Transl. Med.*, 2019, **17**, 124.
- 37 P. A. Baird, T. W. Anderson, H. B. Newcombe and R. B. Lowry, *Am. J. Hum. Genet.*, 1988, **42**, 677–693.
- 38 F. Mouliere, D. Chandrananda, A. M. Piskorz, E. K. Moore, J. Morris, L. B. Ahlborn, R. Mair, T. Goranova, F. Marass, K. Heider, J. C. M. Wan, A. Supernat, I. Hudecova, I. Gounaris, S. Ros, M. Jimenez-Linan, J. Garcia-Corbacho, K. Patel, O. Østrup, S. Murphy, M. D. Eldridge, D. Gale, G. D. Stewart, J. Burge, W. N. Cooper, M. S. Heijden, C. E. Massie, C. Watts, P. Corrie, S. Pacey, K. M. Brindle, R. D. Baird, M. Mau-Sørensen, C. A. Parkinson, C. G. Smith, J. D. Brenton and N. Rosenfeld, *Sci. Transl. Med.*, 2018, **10**, eaat4921–4933.
- 39 S. Cristiano, A. Leal, J. Phallen, J. Fiksel, V. Adleff, D. C. Bruhm, S. Jensen, J. E. Medina, C. Hruban, J. R. White, D. N. Palsgrove, N. Niknafs, V. Anagnostou, P. Forde, J. Naidoo, K. Marrone, J. Brahmer, B. D. Woodward, H. Husain, K. L. Rooijen, M. W. Ørntoft, A. H. Madsen, C. J. H. Velde, M. Verheij, A. Cats, C. J. A. Punt, G. R. Vink, N. C. T. Grieken, M. Koopman, R. J. A. Fijneman, J. S. Johansen, H. J. Nielsen, G. A. Meijer, C. L. Andersen, R. B. Scharpf and V. E. Velculescu, *Nature*, 2019, **570**, 385–391.
- 40 P. Jiang and Y. M. D. Lo, *Trends Genet.*, 2016, **32**(6), 360–371.